Proceedings Paper:

Wilkinson, NJ orcid.org/0000-0003-1506-9900, Lukic-Mann, M, Shuttleworth, MP orcid.org/0000-0002-0538-6438 et al. (2 more authors) (2019) Aerosol Jet Printing for the Manufacture of Soft Robotic Devices. In: 2019 2nd IEEE International Conference on Soft Robotics (RoboSoft). Robosoft 2019, 14-18 Apr 2019, Seoul, South Korea. IEEE , pp. 496-501. ISBN 978-1-5386-9259-2

https://doi.org/10.1109/ROBOSOFT.2019.8722766

Aerosol Jet Printing for the Manufacture of Soft Robotic Devices

Nathan J. Wilkinson, *Student Member, IEEE*, Maria Lukic-Mann, Matthew P. Shuttleworth, Robert W. Kay, and Russell A. Harris

Abstract— **Soft robotics is a fast growing field of engineering where there are significant opportunities to realize new forms of actuation and sensing. However, there is also a challenge to translate some of the lab-based developments into a robust industrial manufacturing process. Linked to this is also the opportunity to create new forms of functionality in soft robotic devices by employing a flexible, digital manufacturing process for their creation. Overcoming these hurdles, and unlocking the possibilities for greater functionality, is likely to be a key enabler for wider applications and adoption of soft robotics in practical applications. We present a system of computer-controlled Aerosol Jet Printing that will enable complex soft robotic structures to be manufactured. The process is demonstrated through the deposition of a carbon-based conductive ink on to elastomeric substrates for high resolution, conformal and multi-layer patterning. Functional demonstrators, in the form of a dielectric elastomer actuator and strain sensor, are produced to showcase the potential of the technique.**

I. Introduction

The translation of soft robotic devices from laboratory demonstrators to real world applications will require significant innovation in design, control and materials science [1]. One of the key drivers in addressing these will be the development of manufacturing processes that enable freeform manufacture and improved functionality[2]. Techniques that remove the geometric limitations of the casting, molding and soft lithographic techniques often used in soft robotics will allow promising design approaches, such as algorithmic design, to be applied without restriction [3]. Improvements in control can be realized through in-situ manufacture of sensors that allow a greater degree of proprioception and environmental awareness for closed-loop operation [4]. Furthermore, we are able to extend the range of materials to create soft robotic structures through manufacturing processes which do not have inherent rheological constraints.

Much of the pioneering work within soft robotics was conducted with manual fabrication and assembly techniques. While they may not hamper low-volume experimental work, it is appreciable that these have restrictions when considering translation towards effective manufacture. These methods would prove to be prohibitively expensive and lack the repeatability required for commercialization at greater scales. Consequently, research groups have begun investigating digitally-driven, automated fabrication techniques to address these problems while also presenting opportunities for increased geometric freedom, mass customization, tool-less manufacture, and decreasing the size scales at which soft robots can be produced.

Early examples used commercially available additive manufacturing equipment to produce soft robotics [5], [6] and, despite material limitations, illustrated the potential of the approach. Techniques capable of depositing the materials usually associated with soft robotics, such as silicone rubbers, soon followed [7], [8]. However, methods that can functionalize soft structures through the printing of sensors, electronics or even catalysts are significantly less prevalent.

Some techniques have begun to illustrate the value that resides in different process approaches [9]. For example, the EMB3D technique, which prints both fugitive and functional inks within an uncured elastomer, was recently used to produce a pneumatic actuator capable of sensing inflation, curvature, contact and even temperature [10].

The development of hybrid manufacturing approaches that combine the material and geometric capabilities of different processes show the most promise [11], [12]. The technique demonstrated here uses Aerosol Jet Printing (AJP) to deposit a functional ink on to the surface of pre-cured elastomer substrates. In addition to the aforementioned arguments for translation to effective manufacturing, the use of this jetting technique provides an opportunity for the soft robotics community to explore new possibilities in terms of design and material composition. As a functionalization technique AJP has a number of advantages: it is compatible with ink viscosities of 1-1000cp [13]; can deposit at distances of 1-5mm from the surface of the substrate [14]; and can produce features ranging from microns to millimeters. Furthermore, the relative independence of the deposition mechanism and substrate mean that AJP is compatible with both existing and emerging strategies for the production of soft robotics.

This paper showcases AJP through the deposition of a stretchable conductive ink on to soft structures. High resolution, conformal and multi-layer patterning are demonstrated; as well as functional components in the form of dielectric elastomer actuators (DEA) and strain sensors. This first application lays the ground work for future manufacturing processes that combine AJP surface

* This research is funded by the Engineering and Physical Sciences Research Council (EPSRC) through grants EP/M026388/1 and EP/L02067X/2

N. J. Wilkinson, M. Lukic-Mann, M. P. Shuttleworth, R. W. Kay and R. A. Harris are members of the Future Manufacturing Process Research Group, University of Leeds, LS2 9JT, United Kingdom (e-mail: mnnjw@leeds.ac.uk)

functionalization with other additive techniques for the integrated, push-button manufacture of soft robotic devices.

II. Aerosol Jet Printing

AJP emerged from DARPA's Mesoscale Integrated Conformal Electronics program that aimed to develop technologies capable of printing circuitry on almost any surface. The capabilities of AJP printing have been widely documented for printed electronics through the production of conformal antenna [15]; interconnects [14]; and even electrical componentry, such as OLEDs [16] and transistors [17]. Colloids, solutions and multi-part materials with viscosities ranging from 1-1000cp have been proven to be compatible with the AJP process, which has made it a major driver behind printed electronics research.

Fundamentally, the process does not differ significantly from any aerosol-based process: a functional ink is suspended in a carrier gas, which is then directed at a substrate that can be articulated relative to the nozzle to produce the desired geometry. More uniquely, high resolution is achieved through the production of a consistent aerosol in combination with an effective focusing mechanism (Figure 1). Depending on the viscosity of the ink, the aerosol can be produced using either ultrasonic (1-10cp) or pneumatic atomisation (10-1000cp). Ultrasonic atomisation produces a series of standing capillary waves at the ink-gas interface. Once these are of sufficient magnitude, they begin to eject droplets in to the carrier gas flow. This approach to atomisation produces a monodisperse aerosol that is suitable for printing.

In contrast, the pneumatic atomizer produces an aerosol with much higher dispersity by using a high-speed gas flow to draw ink from a reservoir. The liquid ink is then sheared to form discrete droplets that are suspended in the carrier gas to form an aerosol. As a result of this high force approach to atomisation, a refinement step is required to produce a printable aerosol. Virtual impaction, a process that splits aerosol streams based on the inertia of the droplets, is required to remove droplets with insufficient inertia for impaction on the substrate.

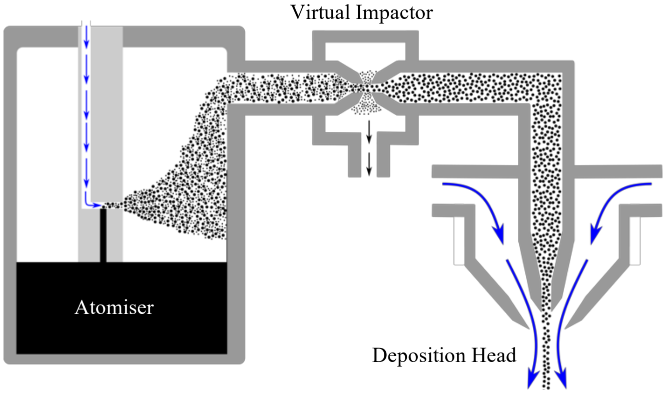

Figure 1 - An Overview of the Aerosol Jet Printing Process

The focusing and deposition of the aerosol is achieved using a combination of a virtual and physical nozzle. The physical nozzle is the predominant factor in determining the scale of the printed feature, with 100μm being the smallest available nozzle. Further focusing can then be accomplished using the virtual nozzle to achieve deposits approaching 10μm [18], [19]. This secondary focusing method works by surrounding the aerosol stream with a sheath gas that both reduces the diameter of the aerosol stream and collimates the aerosol flow. Not only does this improve process resolution, the use of a sheath gas reduces the instances of nozzle clogging as the ink rarely contacts any side walls; enables consistent deposition at stand-off heights of 1-5mm; and allows in-process modification of the effective nozzle diameter by altering the gas flow ratios. These attributes combine to provide a unique opportunity to embed complex actuation, sensing and circuitry within soft robotic devices.

III. Manufacture

This work focusses on the deposition of a carbon-based conductive ink on to three commonly used silicone and acrylic elastomer substrates: Sylgard 184, Elastosil P7670 and 3M VHB 4910. A number of materials were tested to ensure the developed process would be compatible with existing soft robotics materials. The silicone elastomers were processed using both spin coating and casting techniques, while VHB 4910 was purchased as a sheet that was cut and pre-stretched. The strain sensor was manufactured using Elastosil P7670 and the DEA was produced using VHB4910 (3:1 prestrain). All other demonstrators were produced using Sylgard 184 as it has an increased pot life.

All substrate materials were prepared as per the manufacturer's instructions (Sylgard 184, 10:1 & Elastosil P7670, 1:1) and placed in a planetary mixer degasser (Thinky ARE-250) to ensure sufficient mixing and removal of air bubbles. For the cast substrates, the liquid elastomer was then poured in to molds produced using stereolithography (SLA, Formlabs), which were then placed in an oven to ensure the elastomers were sufficiently cured. The final geometry of the strain gauge was achieved by laser cutting the silicone elastomer (Epilog Mini 50W, Epilog Laser, UK)

For spin coating, glass slides were dip-coated in PVA (3%wt aqueous solution) to act as a release layer for the elastomer. The glass slides were then placed in to a spin-coater (SPS, Spin200i, Germany) and a small volume (5ml) of the liquid elastomer was placed on the center of the substrate. Spin coating of elastomeric materials is typically carried out for relatively long times at low speeds, with an initial slow spin to aid in spreading the elastomer. For this process, the elastomer was spun at 1200rpm for 480 seconds. Measurements taken using white-light interferometry (Bruker NPFlex) showed the spin coated elastomer films to have a thickness of approximately 4μm.

Following the manufacture of the base substrates, the silicone elastomers required modification of the surface energy to improve wetting of the printed inks through an oxygen-plasma surface treatment (Plasma Etch, USA). As well as improving wetting characteristics, this approach can enable effective bonding of silicone elastomer structures, as has been recently demonstrated in the field of soft robotics [20].

AJP was achieved through pneumatic atomisation and jetting through a 3mm slotted nozzle for all samples except the high resolution, multilayer device, which was produced using a 300μm circular nozzle. The slotted nozzle allowed increased material flow rates and decreased printing times at the expense of resolution. Toolpaths and G-Code generation for all of the printed deposits was produced from DXF design files using an in-house tool-path generation software designed for continuous printing.

A. Characterization of Printed Lines

AJP is able to produce extremely fine layers, which allows soft robotics to be manufactured at smaller size scales. While this does allow for tunable electrical performance; a consequence of the low layer thickness and the relatively low conductivity of most carbon-based conductive inks is the requirement to build up material through sequential layering or increased throughput.

White light interferometry was used to provide a quantitative assessment of a series of deposits produced using a 3mm slotted nozzle (Figure 3). The thinnest and thickest mean layer height measured during these tests were found to be 345nm and 4.36μm for a single pass and 20 passes, respectively. As predicted, the thickness of the deposit appears to increase linearly with the number of passes of the Aerosol Jet print head.

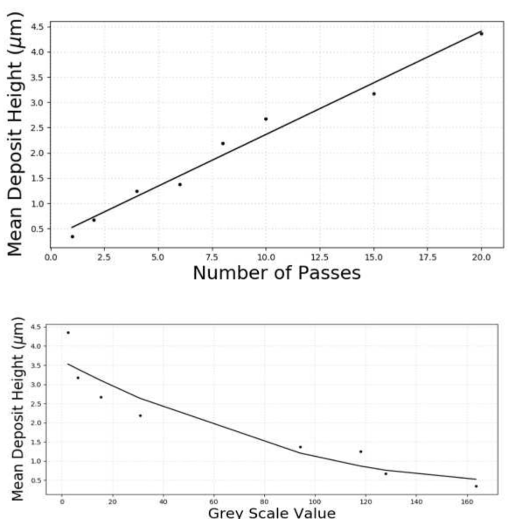

Figure 2 - Mean deposition height of the conductive carbon deposit with an increasing number of passes

Although useful for high resolution quantitative evaluation, interferometry is limited in its use for in-process metrology of the deposit as the time of the scans would severely impact the manufacturing time scales and prohibitively increase machine cost. As a result, assessment using optical microscopy was conducted to investigate its effectiveness at predicting deposition thickness. Image analysis of 80 images showed that mean greyscale was a suitable indicator of both confluency and thickness of the deposit, particularly during the early stages of printing. While limited for highly layered deposits (> 20 layers), this approach shows promise as a relatively simple '*go/no-go*' technique for in-process quality assessment.

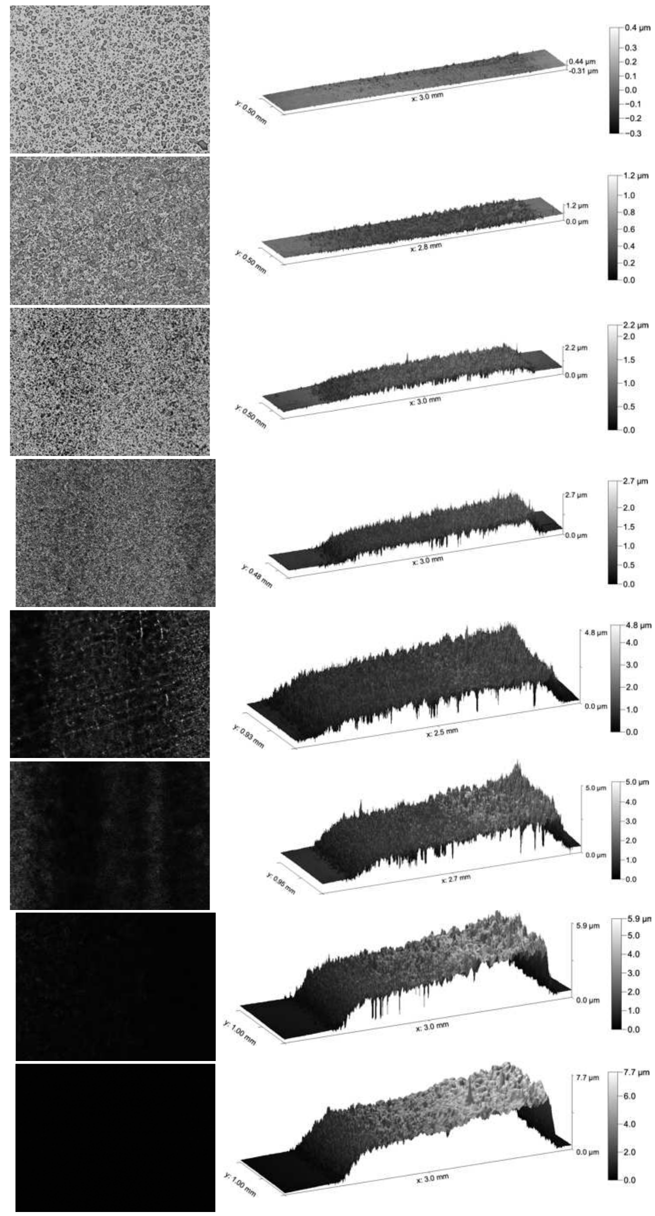

Figure 3 - Optical micrographs and white light interferometry of AJP printed deposits with 3mm slotted nozzle showing changing morphology with increased number of layers

B. High Resolution, Multi-layer Printing

By switching the 3mm slotted nozzle of the Aerosol Jet for a more conventional circular nozzle, it is possible to deposit with high spatial resolution. Using a 300μm nozzle to deposit on to PDMS and glass surfaces, features with an average full width at half maximum (FWHM) height of 25μm where achieved. High variation in line width was observed when printing features on this size, with a 4.3μm standard deviation being observed for the line in Figure 4**.** This has been demonstrated through the production of a 5-layer structure consisting of alternating PDMS and carbon-conductive layers with and overall geometry of 25x75x1mm. The digitally driven nature of AJP means it is very straightforward to vary the geometry of the printed structure on a layer by layer basis, as compared to template-based techniques. The high spatial resolution presented here presents an opportunity to manufacture intelligent soft robotic systems at smaller size scales. Depositing functional inks at high resolution is attractive for a field that is looking towards miniaturized arrays of imprecise sensors for proprioceptive feedback[11].

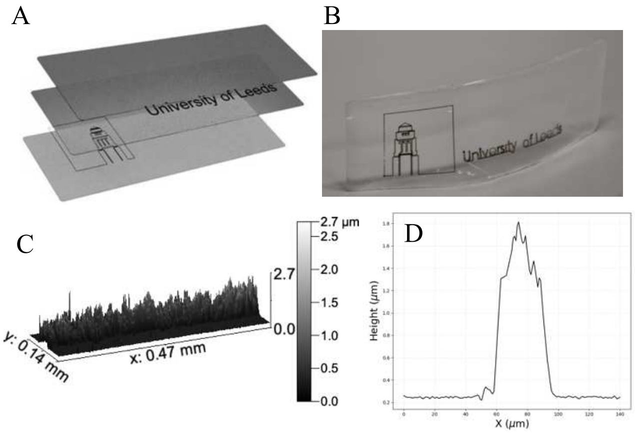

Figure 4 - A) Exploded assembly of multi-layer PDMS and carbon conductive structure, B) Physical part, C) White light interferometry capture of B, D) Typical line profile taken from data in C

C. *Conformal Printing*

Many direct write, or surface functionalization techniques are reliant on close control of the nozzle substrate distance to achieve consistent deposits. As such, printing on conformal surfaces requires more complex articulation and often imposes geometric limitations when trying to produce toolpaths that track a substrate with non-planar geometry. For example, printing on small concave radii can be difficult owing to bulky deposition heads. However, the ability of AJP to deposit consistently at stand-off heights of 1-5mm presents an opportunity to simplify this by reducing the degree to which the motion of the deposition head needs to replicate the surface. Furthermore, as the nozzle does not need to maintain perpendicularity to the surface, printing on to conformal surfaces can be achieved even with relatively simple 3-axis motion systems (Figure 5). By integrating more complex articulation and toolpath planning it is possible to deposit on to almost any substrate geometry.

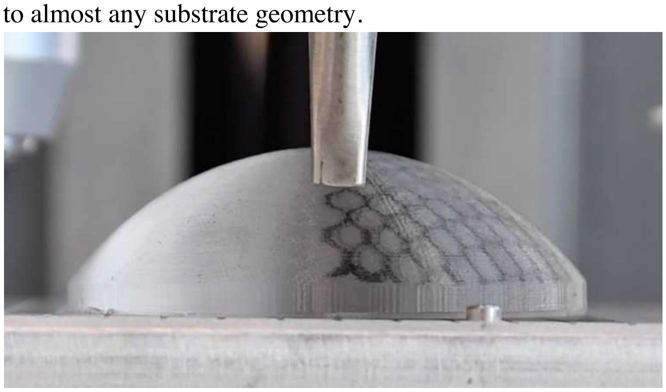

Figure 5 - Aerosol Jet deposit of carbon-based conductive on to a conformal PDMS substrate

IV. Dielectric Elastomer Actuator

Dielectric elastomer actuators were first documented in the late 1990s as an electrically stimulated artificial muscle technology [21], [22]. From this, an entire branch of research has emerged to develop and translate interesting laboratory demonstrators into functional devices. Much of the work in this field has formed around VHB acrylic elastomers owing to their wide availability, relatively low-cost and seemingly high performance. Actuators assembled using this acrylic elastomer have achieved strains exceeding 200% and have been applied to areas as diverse as variable focus lenses [23], audio speakers [24] and haptic feedback devices[25].

A feature of these devices is that the elastomer films require pre-stretch to achieve the highest levels of strains. As a result, the application of electrodes can be challenging as films have a tendency to tear during processing. Furthermore, printing on to the surface of a delicate, suspended film can be challenging for processes that require close control of the nozzle-substrate stand-off. Alternatives to direct write, such as pad printing, have been found to have similar difficulty when depositing on to suspended films[26].

In practice, this means many researchers working with VHB DEAs are still reliant on applying electrodes by hand [27], [28]. AJP provides contactless technique to overcome this challenge as it can provide consistent, high resolution deposits at stand-off heights approaching 5mm. Additionally, as the dielectric elastomer is compressed during actuation, not the conductive itself, the conductive layer should be as thin as possible in order to maximize the overall strain of the device.

To demonstrate this a series of dielectric elastomer actuators were produced (Figure 6) using AJP printing and their strain performance was analyzed using image processing techniques (OpenCV, Nikon D7500, 60fps). The AJP printing process was used to apply electrodes with a diameter of 30mm on the surface of the elastomer film. The DEA was then actuated at voltages ranging from 1kV to 20kV at a frequency of 1Hz using a high-power amplifier (TREK 20/20HS) coupled with a Keithley Function Generator.

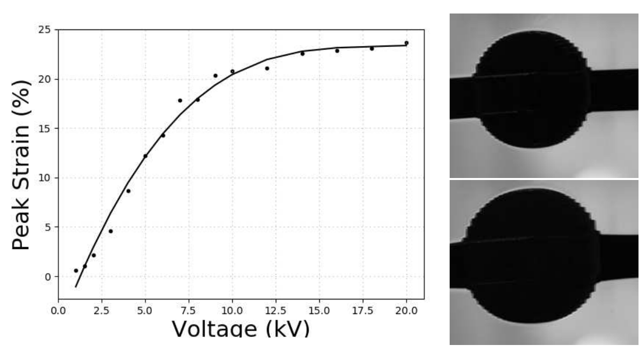

Figure 6 - Strain response of VHB4910 elastomer Actuators with AJP electrodes

As would be expected, strain increased linearly with applied voltage. However, this only occurred up to around 6kV, where the amount of strain began to plateau. At this point, the frequency of actuation was too small relative to the time constant of the actuator. The device was tested up to audible actuation frequencies of around 6kHz, where it continued to perform successfully.

The performance limitations of the dielectric elastomer actuator can largely be attributed to the relatively high resistance of the electrode material. The charge and discharge time of a dielectric elastomer actuator is dependent on the resistance of the electrodes and capacitance of the device. As such, the performance of the device can be improved by increasing the number of printed conductive layers or transitioning to an ink with higher conductivity. Despite this, the DEA presented here performs comparably to those found in the literature, showing that AJP is a viable and promising technique for printing electrodes in dielectric elastomer actuators.

V. Strain Sensor

Effective techniques for manufacturing soft robots with embedded sensing are appealing to achieve more widespread adoption. Positional feedback is typically centered around resistive [29], capacitive [30], or optical sensing. Optical methods have been developed using both wave guides [31] and vision based tracking techniques [32]. Resistive and capacitive techniques generally rely on geometric deformation to alter the electrical performance.

The simple device presented here (Figure 7A) relies on resistance changes to indicate the degree of strain. During testing the device was strained between 0-140% in 10% increments. The sensor was cycled through each set point 100 times and the strain response plotted in Figure 7B. This test was extended to include 150% strain, however at this point continuity errors begin to present within the sensor. A secondary test was carried out that tested the performance of a sensor over 1000 cycles at a 70% strain set point to evaluate any performance drift over time (Figure 7C). The strain sensor presented here is relatively small in size, with a total length of 20mm and an unstrained thickness of 2mm.

The normalized resistance response was found to be stable for any given value of strain and exhibited near linear performance, particularly for strain values below 60%. However, some challenges remain in both the manufacture and characterization of the strain sensing devices. Firstly, the starting resistance (R_0) of different gauges was found to vary significantly (5-30MOhm). Although the reason for this is yet to be quantified, it is possibly a result of inconsistencies in both the printing and assembly process. Connection between the rigid electrodes and soft elastomer was guaranteed through the manual placement of a small amount of conductive carbon grease, which likely had an impact. It is also expected that the resistance of these devices can be decreased by increasing the volume of deposited material. The data collected above was produced by actuating to a set point, taking a series of measurements, and then returning to the unstrained position. This was then repeated for 100 cycles for each value of strain. As such, hysteresis effects have not yet been characterized.

Future work expects to address some of these challenges through optimization and improvements to the manufacturing methodology. A better transition from the rigid and soft components will likely help overcome some of the challenges with inconsistent values for resistance. Additive approaches present an opportunity for this by printing structures with spatially variable and graded stiffness.

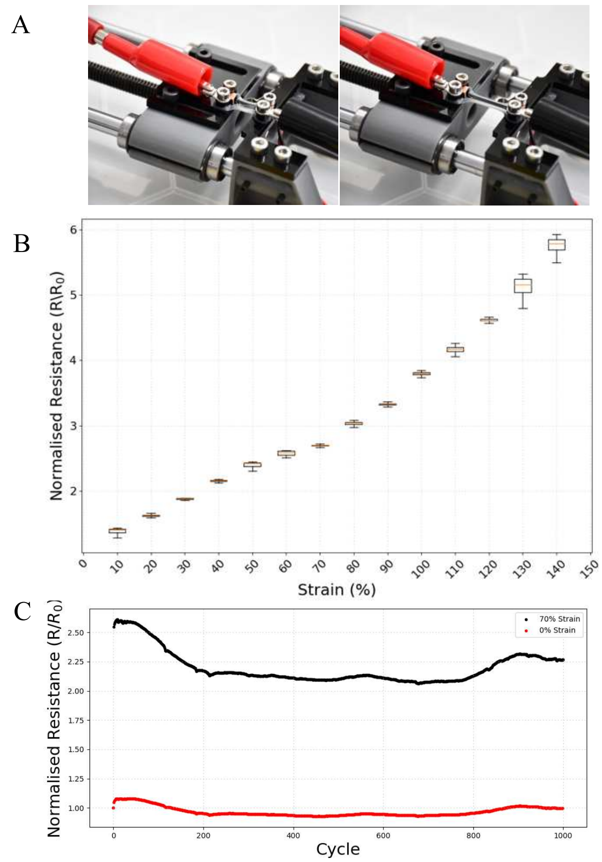

Figure 7 – a) Strain sensor held at 0% and 140% strain b) normalized resistance for 100 readings at various strain set points c) Normalized strain over 1000 cycles at 0% and 70% strain

VI. Conclusion

Aerosol Jet Printing of a carbon-based conductive ink has been demonstrated for embedding functionality within soft robotic devices. This has been illustrated through the creation of a number of devices that highlight the potential impact of AJP in the field of soft robotics.

Inherently digitally driven, the process allows for rapid design changes and layer-by-layer customization of deposit geometry in a way that is difficult or impossible to achieve with conventional template and/or manual processing. This can be realized at resolutions ranging from microns to millimeters, helping to drive the application of soft robotics to challenges at small size scales.

The devices in this research have been produced through the combination of conventional processing (casting, spin coating) and AJP. It demonstrates an opportunity for a hybrid manufacturing approach, in this case by combining surface patterning with additive techniques for the bulk structural geometry. These approaches will enable reliable and repeatable automated manufacture of soft robotics while opening up the possibility for mass customization and condition monitoring. This has significant appeal across a number of new and high-value applications for soft robotics.

Acknowledgment

This research is funded by the Engineering and Physical Sciences Research Council (EPSRC) through grants EP/M026388/1 and EP/L02067X/2.

References

[1] D. Rus and M. T. Tolley, "Design, fabrication and control of soft robots," *Nature*, vol. 521, p. 467, May 2015.

[2] R. L. Truby and J. A. Lewis, "Printing soft matter in three dimensions," *Nature*. 2016.

[3] J. Hiller and H. Lipson, "Automatic design and manufacture of soft robots," *IEEE Trans. Robot.*, 2012.

[4] H. Wang, M. Totaro, and L. Beccai, "Towards Perceptive Soft Robots: Progress and Challenges," *Advanced Science*. 2018.

[5] N. W. Bartlett *et al.*, "A 3D-printed, functionally graded soft robot powered by combustion," *Science (80-.).*, 2015.

[6] T. Umedachi, V. Vikas, and B. A. Trimmer, "Highly deformable 3-D printed soft robot generating inching and crawling locomotions with variable friction legs," in *IEEE International Conference on Intelligent Robots and Systems*, 2013.

[7] T. J. Ober, D. Foresti, and J. A. Lewis, "Active mixing of complex fluids at the microscale," *Proc. Natl. Acad. Sci.*, 2015.

[8] B. N. Peele, T. J. Wallin, H. Zhao, and R. F. Shepherd, "3D printing antagonistic systems of artificial muscle using projection stereolithography," *Bioinspiration and Biomimetics*, 2015.

[9] Y. Yang and Y. Chen, "Innovative Design of Embedded Pressure and Position Sensors for Soft Actuators," *IEEE Robot. Autom. Lett.*, vol. 3, no. 2, pp. 656–663, 2018.

[10] R. L. Truby *et al.*, "Soft Somatosensitive Actuators via Embedded 3D Printing," *Adv. Mater.*, 2018.

[11] T. J. Wallin, J. Pikul, and R. F. Shepherd, "3D printing of soft robotic systems," *Nature Reviews Materials*. 2018.

[12] G.-Z. Yang *et al.*, "The grand challenges of *Science Robotics*," *Sci. Robot.*, 2018.

[13] K. K. B. Hon, L. Li, and I. M. Hutchings, "Direct writing technology-Advances and developments," *CIRP Ann. - Manuf. Technol.*, 2008.

[14] J. A. Paulsen, M. Renn, K. Christenson, and R. Plourde, "Printing conformal electronics on 3D structures with aerosol jet technology," in *FIIW 2012 - 2012 Future of Instrumentation International Workshop Proceedings*, 2012, pp. 47–50.

[15] T. Rahman, L. Renaud, D. Heo, M. Renn, and R. Panat, "Aerosol based direct-write micro-additive fabrication method for sub-mm 3D metal-dielectric structures," *J. Micromechanics Microengineering*, vol. 25, no. 10, p. 107002, Oct. 2015.

[16] J. G. Tait *et al.*, "Uniform Aerosol Jet printed polymer lines with 30 ??m width for 140 ppi resolution RGB organic light emitting diodes," *Org. Electron. physics, Mater. Appl.*, vol. 22, pp. 40–43, 2015.

[17] C. S. Jones, X. Lu, M. Renn, M. Stroder, and W.-S. Shih, "Aerosol-jet-printed, high-speed, flexible thin-film transistor made using single-walled carbon nanotube solution," *Microelectron. Eng.*, vol. 87, no. 3, pp. 434–437, Mar. 2010.

[18] F. Cai, Y.-H. Chang, K. Wang, C. Zhang, B. Wang, and J. Papapolymerou, "Low-Loss 3-D Multilayer Transmission Lines and Interconnects Fabricated by Additive Manufacturing Technologies," *IEEE Trans. Microw. Theory Tech.*, vol. PP, no. 99, 2016.

[19] A. Mahajan, C. D. Frisbie, and L. F. Francis, "Optimization of Aerosol Jet Printing for High-Resolution, High-Aspect Ratio Silver Lines," *ACS Appl. Mater. Interfaces*, vol. 5, no. 11, pp. 4856–4864, Jun. 2013.

[20] T. Ranzani, S. Russo, N. W. Bartlett, M. Wehner, and R. J. Wood, "Increasing the Dimensionality of Soft Microstructures through Injection-Induced Self-Folding," *Adv. Mater.*, 2018.

[21] R. E. Pelrine, R. D. Kornbluh, and J. P. Joseph, "Electrostriction of polymer dielectrics with compliant electrodes as a means of actuation," *Sensors Actuators A Phys.*, vol. 64, no. 1, pp. 77–85, 1998.

[22] R. Pelrine, "High-Speed Electrically Actuated Elastomers with Strain Greater Than 100%," *Science (80-.).*, vol. 287, no. 5454, pp. 836–839, Feb. 2000.

[23] L. Maffli, S. Rosset, M. Ghilardi, F. Carpi, and H. Shea, "Ultrafast all-polymer electrically tunable silicone lenses," *Adv. Funct. Mater.*, vol. 25, no. 11, pp. 1656–1665, 2015.

[24] C. Keplinger, J.-Y. Sun, C. C. Foo, P. Rothemund, G. M. Whitesides, and Z. Suo, "Stretchable, Transparent, Ionic Conductors," *Science (80-.).*, vol. 341, no. 6149, pp. 984–987, 2013.

[25] H. Phung *et al.*, "Interactive haptic display based on soft actuator and soft sensor," in *IEEE International Conference on Intelligent Robots and Systems*, 2017.

[26] S. Rosset and H. Shea, "Towards fast, reliable, and manufacturable DEAs: Miniaturized motor and Rupert the rolling robot," in *Proceedings of SPIE - The International Society for Optical Engineering*, 2015, vol. 9430, no. January.

[27] K. M. Digumarti, C. Cao, J. Guo, A. T. Conn, and J. Rossiter, "Multi-directional crawling robot with soft actuators and electroadhesive grippers," in *2018 IEEE International Conference on Soft Robotics, RoboSoft 2018*, 2018.

[28] A. Fishman, S. Catsis, M. Homer, and J. Rossiter, "Touch and see: Physical interactions stimulating patterns in artificial cephalopod skin," in *2018 IEEE International Conference on Soft Robotics, RoboSoft 2018*, 2018.

[29] J. T. Muth *et al.*, "Embedded 3D printing of strain sensors within highly stretchable elastomers," *Adv. Mater.*, 2014.

[30] M. C. Yuen, R. Kramer-Bottiglio, and J. Paik, "Strain sensor-embedded soft pneumatic actuators for extension and bending feedback," in *2018 IEEE International Conference on Soft Robotics, RoboSoft 2018*, 2018.

[31] H. Zhao, K. O'Brien, S. Li, and R. F. Shepherd, "Optoelectronically innervated soft prosthetic hand via stretchable optical waveguides," *Sci. Robot.*, 2016.

[32] C. Chorley, C. Melhuish, T. Pipe, and J. Rossiter, "Development of a Tactile Sensor Based on Biologically Inspired Edge Encoding," in *International Conference on Advanced Robotics*, 2009.